MET5471 – Sat. Remote Sensing of PA 11/23/2024
Cansu Duzgun

MET5471 Project II: Wave Interaction with water and ice particles

This project aims to understand how particles scatter and absorb electromagnetic wave (EM) energy. It is important to understand because we use this information in the remote sensing applications of aerosols, clouds, and precipitation. Under the influence of the external EM waves, the originally neutral materials become "electrically polarized". There are two different types and three different mechanisms for polarization. In the case of H_2O, induced polarization is driven by an atomic mechanism in the infrared (IR) spectrum, while the re-orientation of permanent dipoles occurs via the orientation mechanism in the microwave (MW) spectrum. These polarizations allow H_2O particles to interact with EM waves by scattering and absorbing them.

Water and ice are the most important materials for remote sensing because at the surface we have oceans, sea ice, and snow cover; and in the atmosphere, we have rain and precipitating ice. To be able to estimate their emission, absorption, and reflection we need to know 'refractive indices' – m. The refractive index m=n-ik characterizes how light interacts with a material. Here, n represents the real part that governs the *speed and bending of light*, while k, the imaginary part, quantifies the *absorption of light within the material*. The refractive indices of water and ice are computed in this project using a Python code that is written by Dr. Guosheng Liu, based on Ellison (2007) for water in the microwave and far-infrared, Hale and Querry (1973) for water in the visible and infrared, Warren and Brandt (2008) for ice in the visible and infrared, and Mätzler (2006) for ice in the microwave.

When particle size 'r' is much smaller than the wavelength of the wave, we may approximate that the electric field within the particle is uniform, and the particle is a single oscillating dipole – this is 'Rayleigh scattering'. When 'r' becomes large (compared to wavelength), it is no longer valid to assume that the electric field inside the particle is constant. The large particle is an aggregate of the number of small particles, these are multiple dipoles. The scattered field can be considered a superposition of all scattered fields of these small particles – this is "Mie scattering". In this project, we will model the Mie scattering of spherical water drops and ice spheres.

Mie theory assumes that the particle is a homogeneous sphere, and the incident light is a monochromatic plane wave. However, not all particles are homogeneously spherical. In the introduction of Wiscombe's technical note (1979), this is explained with these sentences "While vast majority of scattering particles are not spherical, so that the Mie solution does not strictly apply to them, both intuition, and experimental evidence (e.g., Zerull 1976) indicate that, with

averaging over orientation and/or size, mildly non-spherical particles scatter very much like 'equivalent' spheres. This, of course, vastly enhances the utility of Mie solution."

'Extinction' can be defined as the decrease in density by absorption and scattering. Suppose we consider radiation as a stream of photons that flow into a volume containing the scattering particle. In that case, each particle blocks a certain amount of photons, resulting in a reduction of transmitted radiation. This blocking can be considered in two parts: 1) absorption: where photons disappear and later reappear at different frequencies, and 2) scattering: diverted into other directions. The efficiency of this blocking can be calculated by dividing the extinction cross-section (which depends on size, shape, refractive index (m), and wavelength (λ)) by $\pi*r^2$; and it's called 'extinction efficiency'. Mie theory is used to calculate extinction, scattering, and absorption efficiency, following the procedure described by Wiscombe. We used the formulas below.

$$Q_{ext} = \frac{2}{x^2}\sum_{n=1}^{\infty}(2n+1)Re(a_n + b_n)$$

$$Q_{sca} = \frac{2}{x^2}\sum_{n=1}^{\infty}(2n+1)(|a_n|^2 + |b_n|^2)$$

$$Q_{abs} = Q_{ext} - Q_{sca}$$

$$a_n = \frac{(\frac{A_n}{m}+\frac{n}{x})Re(W_n)-Re(W_{n-1})}{(\frac{A_n}{m}+\frac{n}{x})W_n - W_{n-1}} ; b_n = \frac{(mA_n+\frac{n}{x})Re(W_n)-Re(W_{n-1})}{(mA_n+\frac{n}{x})W_n - W_{n-1}}$$

$$A_0 = cot(mx) ; A_n = -\frac{n}{mx} + [\frac{n}{mx} - A_{n-1}]^{-1}$$

$$W_0 = sin(x) + icos(x) ; W_{-1} = cosx - isin(x) ; W_n = (\frac{2n-1}{x})W_{n-1} - W_{n-2}$$

In these formulas, we defined the size parameter 'x' as:

$$x = \frac{circumference\ of\ sphere}{wavelength} = \frac{2*\Pi*r}{\lambda}$$

Also, to be able to find the maximum N needed to add, we used Wiscombe's formula:

$$N = x + 4.05x^{1/3} + 2$$

In Figure 1, we see scattering efficiency (Q_{sca}), extinction efficiency (Q_{ext}), and absorption efficiency (Q_{abs}) for visible light (VIS) at 0.65 μm, when the spherical water drop's size parameter varies from 0.1 to 60. In this case, the first thing that we need to point out is that Q_{ext} and Q_{sca} are nearly identical because Q_{abs} is so small. Q_{ext} is the summation of Q_{abs} and Q_{sca}. Q_{abs} is so small because, in refractive index (m), k is small. For 0.65 μm, m=n-ik is m=1.331-i1.64e-08; which means k = 1.64e-08.

The second important property of graphs in Figure 1 to explain is the Q_{ext} curve for a water droplet, it has several features. First, a series of regularly spaced broad maxima and minima called the *'interference structure'* is present, which oscillates approximately about the value 2; second, an irregular fine structure called *'ripple structure'* is present. We will briefly consider each of these in turn. The '*interference structure'* refers to the broad oscillations caused by constructive and destructive interference of light scattered from different paths around and within the particle, with its periodicity linked to the size parameter. Larger size parameters lead to finer oscillations as the wavelength becomes small compared to the particle size, as can be seen in Figure 1. The *'ripple structure'* consists of finer oscillations superimposed on the interference pattern. Multiple dipoles contribute to the scattered field, creating a fine ripple structure.

The third important property to discuss is reddening and blueing. When $x << 1$, Q_{ext} increases and reddening happens, which means sunlight looks red when passing through the atmosphere (sunset) with clouds and aerosols. When $x >> 1$, Q_{ext} decreases, for blueing to happen particles must be uniform in size. For particles with a wide-spread size spectrum, blueing goes away. Blueing and ripples disappear as the particles are more diversified.

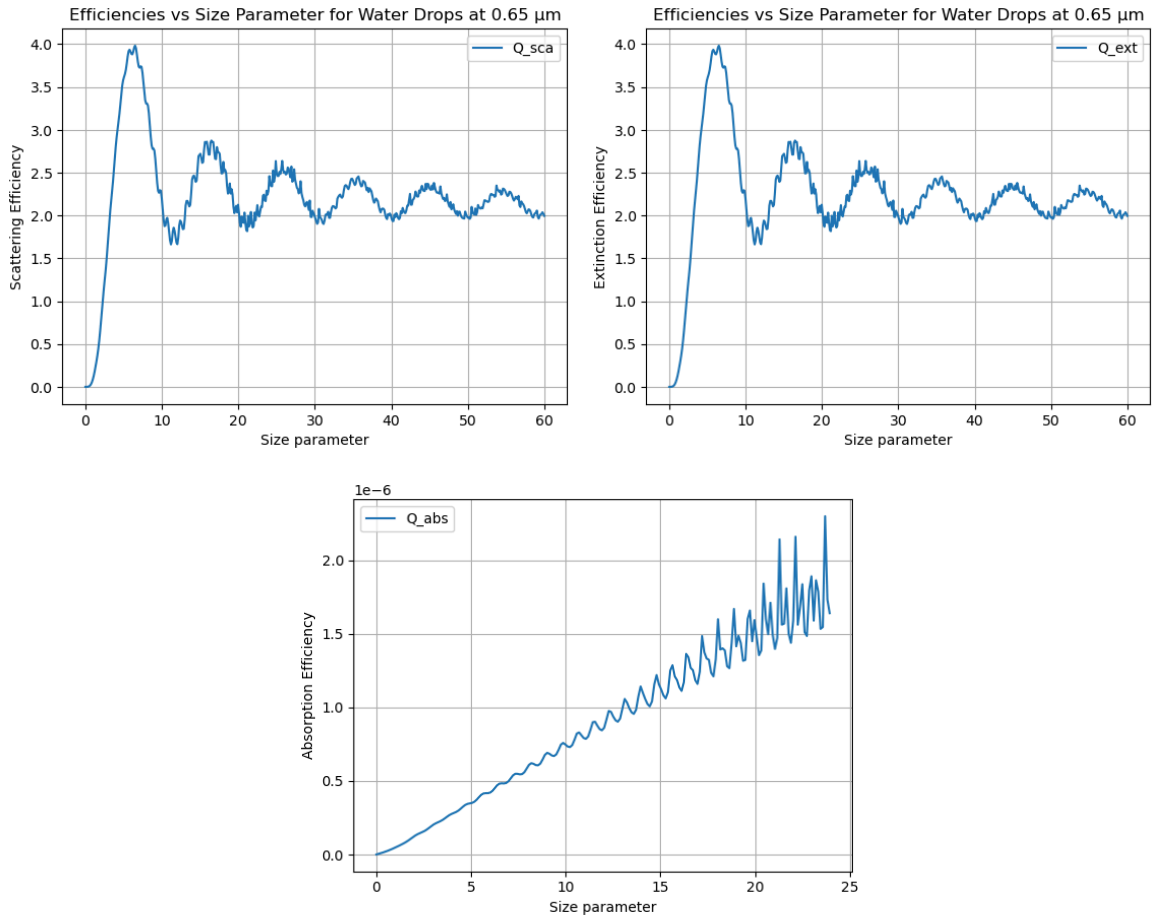

Fig. 1. Extinction, scattering, and absorption efficiency with respect to the size parameter for a pure water droplet.

In Figure 2, we are repeating the above computation by artificially assigning k = 0.1 in refractive index m=n-ik → m=n-i(0.1). As discussed before, larger k will increase absorption by particles, because the imaginary part k determines how much light is absorbed by particles. These graphs are mimicking a heavily polluted water drop. If we compare the pure water case and this case, a small k (was k = 1.64e-08) leads to negligible absorption, yielding efficiency values in the order of 1e-6. Conversely, when k is manually set to mimic polluted air (k = 0.1), the higher imaginary part leads to significant absorption, increasing the efficiency values to a realistic range for polluted particles. Since Q_{abs} is increased this causes Q_{sca} to decrease. The ripples are gone in Q_{ext}, but it continues to approach 2.

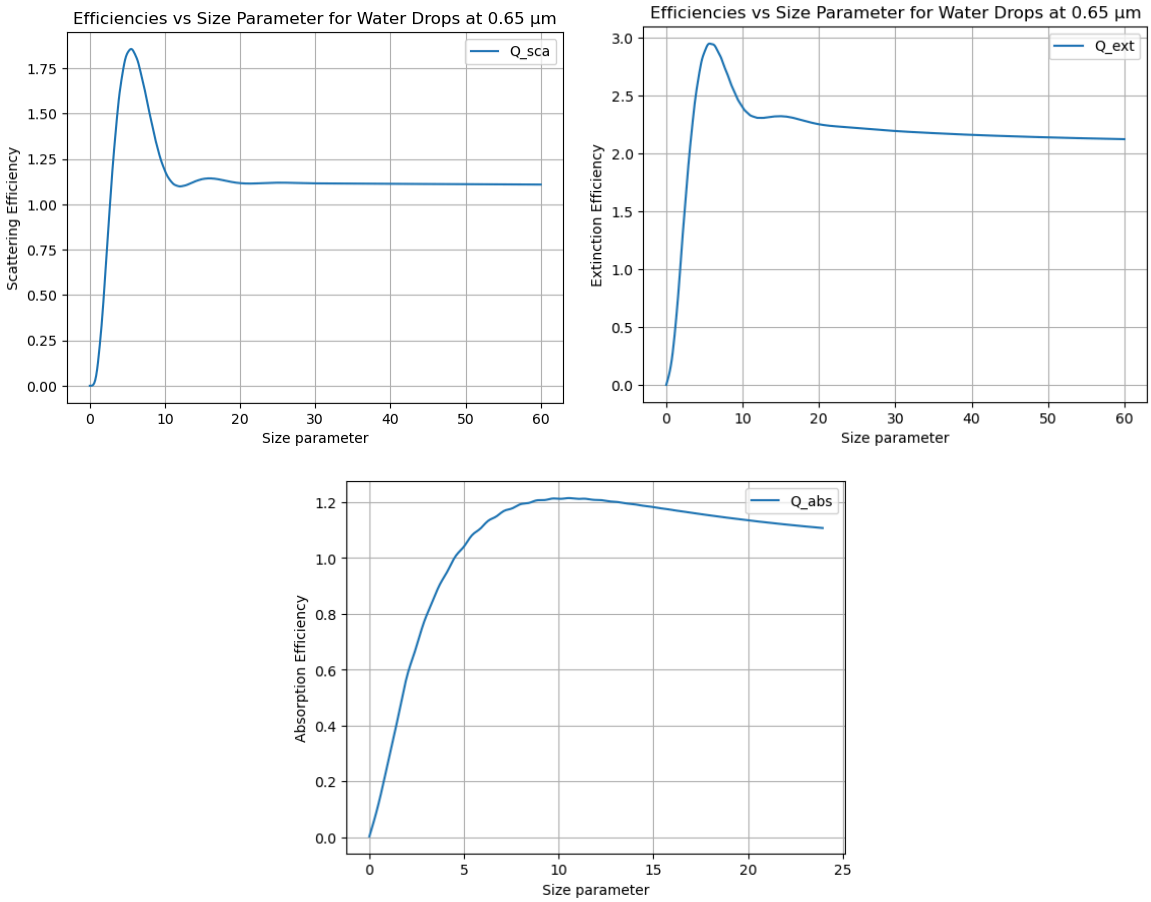

Fig. 2. Extinction, scattering, and absorption efficiency with respect to the size parameter for a heavily polluted water droplet.

We know that for the MW region, k of ice is three orders smaller than water, therefore in this region absorption/ emission is negligible for ice. That's why this region can be used to estimate the liquid water amount. In Table 1, there are comparative values of Q_{sca} and Q_{abs} for water and ice drop with a radius of 20 µm at 37 GHz (MW region), and temperature of 0 °C. As we discussed before, the Q_{sca} quantifies how much of the incident radiation is scattered by the particle. Ice particles scatter slightly less than water particles at this frequency. Both values are very small, indicating that scattering is relatively insignificant at MW wavelengths. The Q_{abs} quantifies how much of the incident radiation is absorbed by the particle. Water absorbs MW radiation far more efficiently than ice (by almost three orders of magnitude), which supports the first sentence of this paragraph, and because of this difference, it is crucial for remote sensing.

To sum up, at 37 GHz, liquid water dominates the microwave signal due to its significantly higher Q_{abs} compared to ice. This makes MW remote sensing highly sensitive to the liquid water content in mixed-phase clouds while being less effective at detecting ice, which absorbs and scatters much less efficiently. Scattering is negligible for both water and ice at this frequency.

Table 1. Q_{sca} and Q_{abs} values for water and ice drop with a radius of 20 μm at 37 GHz, T = 0 °C.

Q_{sca_water}	1.3483072673e-07
Q_{sca_ice}	0.2744972961e-07
Q_{abs_water}	66920.6511282880e-07
Q_{abs_ice}	235.6575196120e-07

As scattering occurs, the scattered energy goes in all directions but is not distributed uniformly. To describe the angular distribution of the scattered energy, a function, called the 'phase function' is introduced: P(Θ). To calculate P(Θ), we used the formulas below:

$$P(\Theta) = 4\Pi * \frac{|S(\Theta)|^2}{k^2 * C_{sca}}$$

$$g = \frac{4}{Q_{sca} * x^2}\left[\sum_{n=1}^{\infty} \frac{n(n+1)}{n+1} Re\{a_n a_{n+1}^* + b_n b_{n+1}^*\} + \sum_{n=1}^{\infty} \frac{2n+1}{n(n+1)} Re\{a_n b_n^*\}\right.$$

$$S(\Theta) = 0.5 * |S_1(\Theta)|^2 + |S_2(\Theta)|^2$$

$$S_1(\Theta) = \sum_{n=1}^{\infty} \frac{2n+1}{n(n+1)} (a_n \Pi_n + b_n \tau_n) ; S_2(\Theta) = \sum_{n=1}^{\infty} \frac{2n+1}{n(n+1)} (a_n \tau_n + b_n \Pi_n)$$

$$a_n = \frac{(\frac{A_n}{m} + \frac{n}{x}) Re(W_n) - Re(W_{n-1})}{(\frac{A_n}{m} + \frac{n}{x}) W_n - W_{n-1}} ; b_n = \frac{(mA_n + \frac{n}{x}) Re(W_n) - Re(W_{n-1})}{(mA_n + \frac{n}{x}) W_n - W_{n-1}}$$

$$A_0 = cot(mx) ; A_n = -\frac{n}{mx} + \left[\frac{n}{mx} - A_{n-1}\right]^{-1}$$

$$W_0 = sin(x) + icos(x) ; W_{-1} = cosx - isin(x) ; W_n = (\frac{2n-1}{x}) W_{n-1} - W_{n-2}$$

$$\Pi_0 = 0 ; \Pi_1 = 1 ; \Pi_n = \frac{2n-1}{n-1} * \mu * \Pi_{n-1} - \frac{n}{n-1} * \Pi_{n-2} ; \mu = \cos\Theta$$

$$\tau_n = n * \mu * \Pi_n - (n+1) * \Pi_{n-1}$$

$$x = \frac{circumference\ of\ sphere}{wavelength} = \frac{2*\Pi*r}{\lambda} ; N = x + 4.05x^{1/3} + 2$$

The general relationship of scattering vs particle size is shown in Figure 3 and four different case properties are listed in Table 2. Graphs in Figures 4 and 5 illustrate the phase functions for water droplets of varying sizes and wavelengths, highlighting the scattering behavior under different conditions.

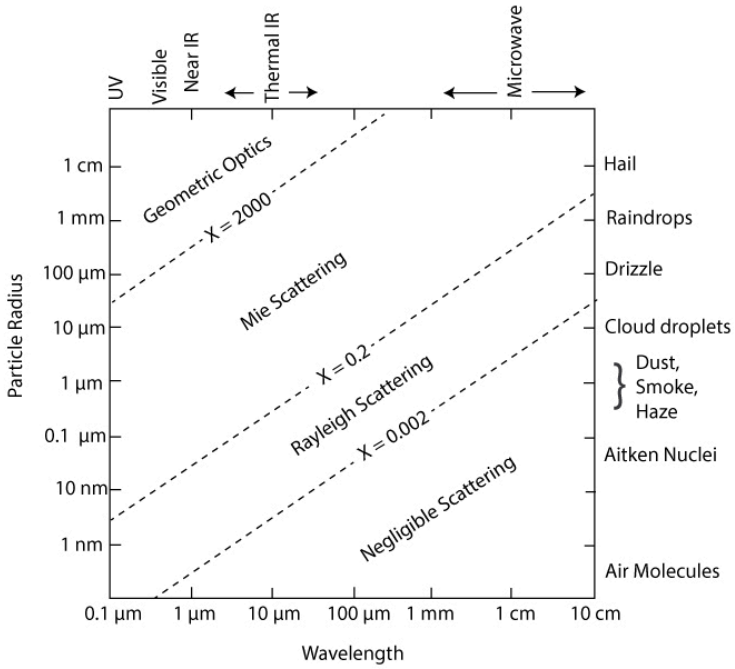

Fig. 3. Relationship of scattering vs particle size.

Table 2. Properties of each case that is evaluated.

Case #	Wavelength (λ)	Radius (r)	Size parameter (x)
Case 4.1.	30 GHz ≈ 1000 µm	10 µm	~0.06
Case 4.2.	30 GHz ≈ 1000 µm	1000 µm	~6
Case 4.3.	0.5 µm	1 µm	~12.5
Case 4.4.	0.5 µm	1000 µm	~12566

In Figure 4, for small droplets, such as in Case 4.1 (r=10 µm, λ=30 GHz), the phase function is nearly symmetric with minimal directional preference. This corresponds to Rayleigh scattering, where the droplet size is much smaller than the wavelength. The asymmetry parameter (g≈0) reflects the nearly isotropic scattering behavior typical of such conditions. Conversely, in Case 4.2 (r=1000 µm, λ=30 GHz), the larger droplet size should've led to

dominant forward scattering, however not yet strongly forward-scattered because the size parameter is not large enough to fully enter the geometric optics regime.

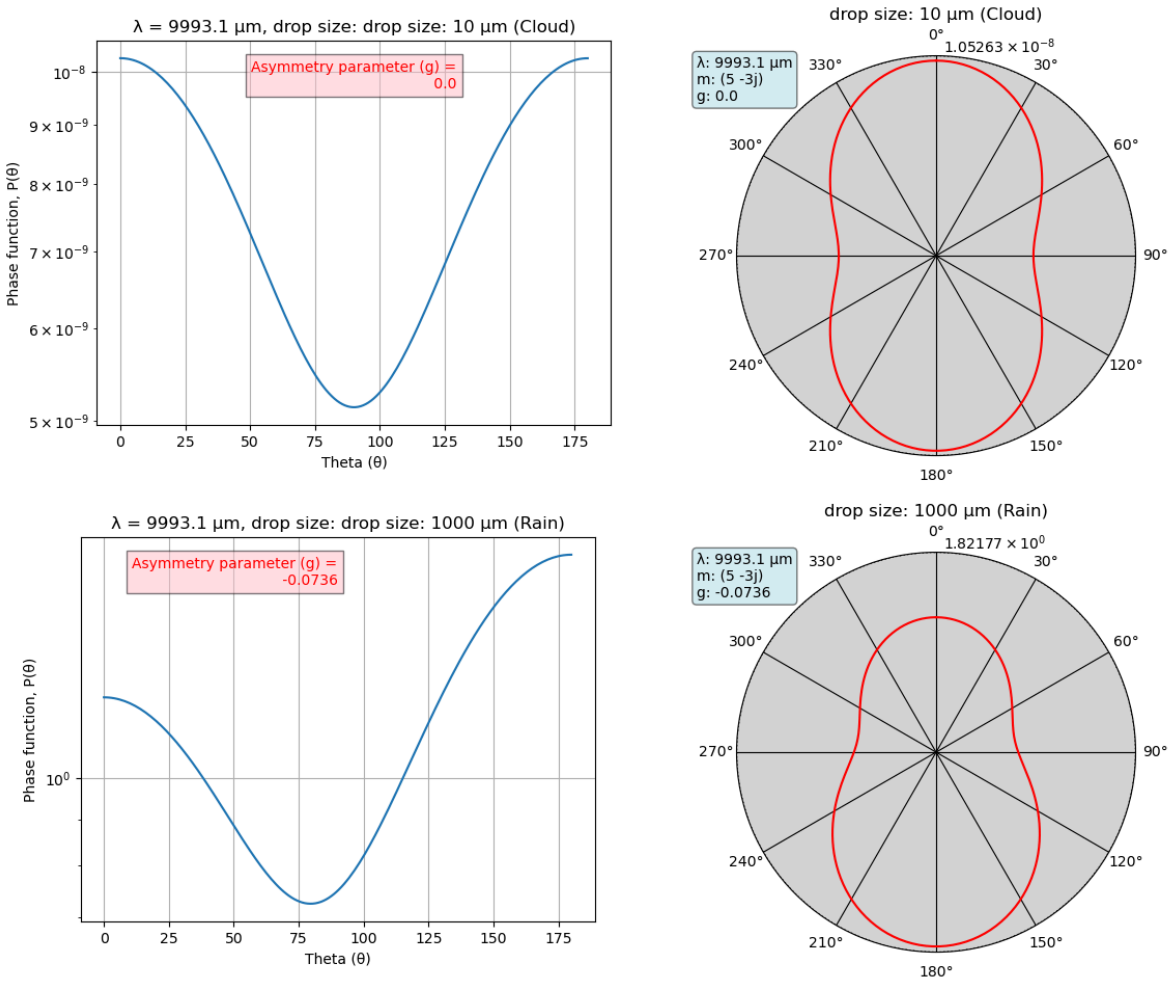

Fig. 4. Phase function for Θ=0 to 180 (μ=1 to -1) degrees with corresponding asymmetry parameter in the red box on the left column, and phase function with r values on a log scale for Θ=0 to 360 degrees for 30 GHz, refractive index, and asymmetry parameter in the blue box on the polar orbit.

In Figure 5, the scattering behavior is strongly influenced by the size parameter x, which is large for both small and large droplets. As the droplet size increases, the size parameter becomes extremely large, and geometric optics effects such as diffraction and constructive interference concentrate nearly all the scattered energy in the forward direction, with minimal scattering in other directions.

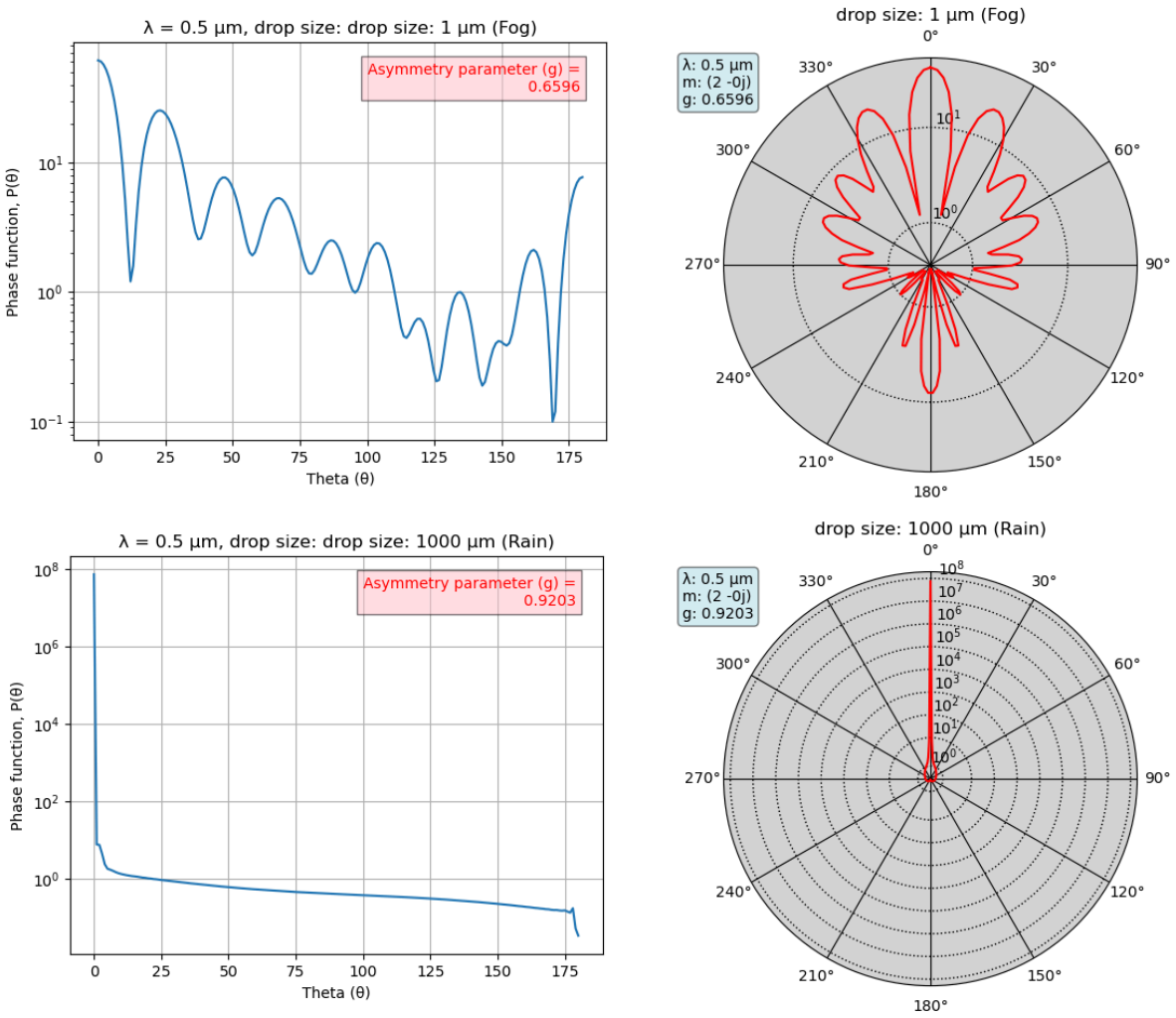

Fig. 5. Phase function for Θ=0 to 180 (μ=1 to -1) degrees with corresponding asymmetry parameter in the red box on the left column, and phase function with r values on log scale for Θ=0 to 360 degrees for 0.5 μm, refractive index, and asymmetry parameter in the blue box on the polar orbit.

Lastly, the asymmetry parameter (g) (values of 'g' can be seen from small boxes in Figures 4 and 5) quantifies the directional bias of scattering and it ranges from -1 (purely backward scattering) to +1 (purely forward scattering), with g = 0 indicating isotropic scattering. 'g' highlights the transition between scattering regimes. In the visible range, increasing droplet size leads to progressively stronger forward scattering, reflected by higher g values. In contrast, in the microwave range, g remains small or slightly negative due to the dominance of Rayleigh scattering for small droplets and weak Mie scattering effects for larger droplets. This shows how g depends on the size parameter and the wavelength of the incident radiation.

References

Ellison, W. J., 2007: Permittivity of pure water, at standard atmospheric pressure, over the frequency range 0–25 THz and the temperature range 0–100°C. *J. Phys. Chem. Ref. Data,* 36, doi:10.1063/1.2360986.

Hale, G. M., and M. R. Querry, 1973: Optical constants of water in the 200-nm to 200-μm wavelength region. *Appl. Opt.,* 12 (3), 555–563, doi:10.1364/AO.12.000555.

Mätzler, C. (2006), Microwave dielectric properties of ice, in Thermal Microwave Radiation—Applications for Remote Sensing, Electromagn, Waves Ser., vol. 52, edited by C. Mätzler et al., chap. 5, 455 – 462, Inst. Eng. Technol., Stevenage, U. K.

Warren, S. G., and R. E. Brandt, 2008: Optical constants of ice from the ultraviolet to the microwave: A revised compilation. *J. Geophys. Res.,* 113, D14220, doi:10.1029/2007JD009744.

Wiscombe, W. J., 1979: Mie scattering calculations: advances in technique and fast, vector-speed computer codes. NCAR/TN-140+STR, 98, https://opensky.ucar.edu/islandora/object/technotes:232.

Zerull, R. H., 1976: Scattering measurements of dielectric and absorbing nonspherical particles. Beitr. Phys. Atmos., 49, 166-188.